

Visible-Light-Driven Photoisomerization and Increased Rotation Speed of a Molecular Motor Acting as a Ligand in a Ruthenium(II) Complex

Sander J. Wezenberg,* Kuang-Yen Chen, and Ben L. Feringa*

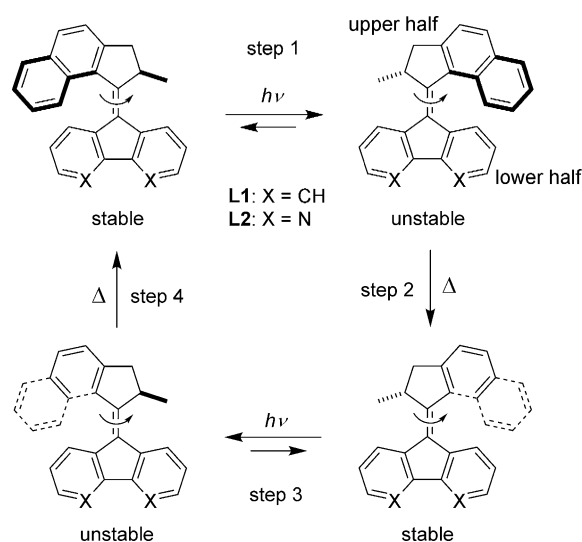
Abstract: Toward the development of visible-light-driven molecular rotary motors, an overcrowded alkene-based ligand and the corresponding ruthenium(II) complex is presented. In our design, a 4,5-diazafluorenyl coordination motif is directly integrated into the motor function. The photochemical and thermal isomerization behavior has been studied by UV/Vis and NMR spectroscopy. Upon coordination to a Ru^{II} bipyridine complex, the photoisomerization process can be driven by visible ($\lambda_{\text{max}} = 450 \text{ nm}$) instead of UV light and furthermore, a large increase of the speed of rotation is noted. DFT calculations point to a contraction of the diazafluorenyl lower half upon metal-coordination resulting in reduced steric hindrance in the “fjord region” of the molecule. Consequently, it is shown that metal-ligand interactions can play an important role in the adjustment of both photophysical and thermodynamic properties of molecular motors.

Photoresponsive molecular switches and motors are emerging as fascinating tools for controlling the properties of smart materials,^[1,2] as well as biological functions.^[3] One of the major hurdles at present, however, is that the molecules most widely applied, that is, azobenzenes,^[4] diarylethenes,^[5] spiropyrans,^[6] and overcrowded alkenes,^[7] are typically operated with UV light. UV irradiation can also trigger highly undesired side processes such as material degradation and cellular apoptosis. One of the key challenges for scientists in the field of photochromic switches is therefore to shift the excitation wavelength to the visible range.

Several strategies toward photoswitching at longer wavelength have been reported.^[8] These include changing the substituent pattern^[9] and BF₂ coordination^[10] in azo compounds, as well as the attachment of aromatic dyes to diarylethenes.^[11] The most widely applied approach though, is by coordination to transition-metal complexes, which can act as photosensitizers.^[12] This process is not trivial, since it can also lead to a perturbation of the excited state properties of the switching unit.^[13] Nevertheless, this approach was successfully used for the visible-light-induced photoisomerization of azobenzenes,^[14] diarylethenes,^[15] spiropyrans,^[16]

a rhodopsin-based switch,^[17] and a rotaxane-derived linear motor.^[18]

Overcrowded alkene-based molecular motors,^[19] developed in our research group, are unique among photoresponsive systems in the sense that their thermal isomerization follows a helix inversion pathway, that is, the upper and lower halves of the molecule flip relative to each other (Scheme 1).



Scheme 1. Isomerization behavior of second-generation overcrowded alkene-based motors with fluorenyl **L1**^[20] and 4,5-diazafluorenyl **L2** lower halves.

Hence, upon repeated photochemical and thermal isomerization steps, the upper half completes a full 360° unidirectional rotary cycle with respect to the lower half. In the past, we have put considerable effort into fine-tuning the speed of rotation by structural modifications.^[20] Our second-generation molecular motors that have a fluorenyl-based lower half (Scheme 1) are among the fastest reported to date.^[19,20] With respect to altering the excitation wavelength, we have recently shown that a substituted analogue of **L1** could be isomerized with visible light by energy transfer from a Pd^{II} porphyrin.^[21] Whereas these studies were based on changes in molecular design using different synthetic strategies, the development of molecular motors as ligands to form metal complexes has not yet been reported to date.

The synthesis and characterization of metallo-based sterically overcrowded alkenes has been described earlier by us^[22] and the group of Belser.^[23] In the latter example, a 4,5-diazafluorenyl coordination motif was introduced and Ru^{II},

* Dr. S. J. Wezenberg, Dr. K.-Y. Chen, Prof. Dr. B. L. Feringa
 Stratingh Institute for Chemistry
 University of Groningen
 Nijenborgh 4, 9747 AG, Groningen (The Netherlands)
 E-mail: s.j.wezenberg@rug.nl
 b.l.feringa@rug.nl

Supporting information for this article is available on the WWW under <http://dx.doi.org/10.1002/anie.201505781>.

Os^{II}, and Re^I complexes were successfully prepared. However, studies on the photochromism of these compounds have not been reported to date. We envisioned that metal coordination to molecular motor **L2** with an intrinsic 4,5-diazafluorenyl ligation motif could offer a viable method to alter the rotary motion and light-absorption properties, without requiring tedious synthetic work.

Herein, we describe the synthesis and characterization of **L2** and its Ru^{II} bipyridine (bpy) complex [Ru(bpy)₂(**L2**)](PF₆)₂. The isomerization behavior of **L2** is shown to be comparable to that of **L1**. Upon ligation to a Ru^{II} center, the photoisomerization process can be triggered by visible light ($\lambda_{\text{max}} = 450$ nm) and a 50-fold increase of the rotation speed is observed. On the basis of the present results, we foresee that metal–ligand interactions will play an important role in future adjustments of both the photophysical and thermodynamic properties of overcrowded alkene-based molecular motors.

Compound **L2** was prepared by subjecting the respective thioketone^[24] and diazo^[24] precursors to a Barton–Kelllogg coupling in refluxing THF (see the Supporting Information for details). The product, isolated in 52 % yield as a racemate, was subsequently stirred under reflux in ethanol with *cis*-[Ru(bpy)₂Cl₂]. Counteranion exchange using ammonium hexafluorophosphate resulted in precipitation of [Ru(bpy)₂(**L2**)](PF₆)₂, which was collected by filtration (61 %) and used as a mixture of diastereomers (that is, Λ -(*R*), Λ -(*S*), Δ -(*R*), Δ -(*S*)).

The photochemical and thermal isomerization behavior of **L2** and [Ru(bpy)₂(**L2**)](PF₆)₂ was studied in degassed CH₂Cl₂ by using low-temperature UV/Vis spectroscopy. Irradiation of **L2** at –20 °C with UV light ($\lambda_{\text{max}} = 365$ nm) resulted in a bathochromic shift of the absorption maximum from 390 nm to 415 nm (Figure 1A). By analogy with structurally related overcrowded alkenes, for example **L1**, this shift indicates the formation of the unstable isomer (Scheme 1).^[19,25]

The UV/Vis absorption spectrum of [Ru(bpy)₂(**L2**)](PF₆)₂ shows maxima around 290, 425, and 450 nm (Figure 1B), which are characteristic for Ru^{II} bpy complexes.^[26] The highest-energy absorption band stems from ligand-centered (LC) $\pi \rightarrow \pi^*$ transitions, whereas the remaining two bands are assigned as metal-to-ligand charge transfer (MLCT) $d\pi \rightarrow \pi^*$ transitions. Similar to **L2**, UV irradiation ($\lambda_{\text{max}} = 365$ nm; $T = -30$ °C) resulted in a red-shifted absorption spectrum, although it was less prominent. Interestingly, excitation into the MLCT absorption bands using 450 nm visible light gave rise to similar spectral changes.^[27] The spectrum of the unbound ligand **L2** on the other hand, did not alter upon 450 nm irradiation. The photoisomerization wavelength could thus be extended from the UV to the visible region upon coordination to Ru^{II}.

[Ru(bpy)₃]²⁺ complexes show broad luminescence around $\lambda = 600$ nm upon MLCT excitation.^[26] For [Ru(bpy)₂(**L2**)](PF₆)₂, this luminescence is quenched (Figure S4 in the Supporting Information), which may tentatively be attributed to energy transfer from the metal complex to the motor.

The samples were irradiated until no further changes in the UV/Vis absorption spectra were noted, that is, the photostationary state (PSS) was reached. Clear isosbestic points were observed (Figures S5–S7 in the Supporting

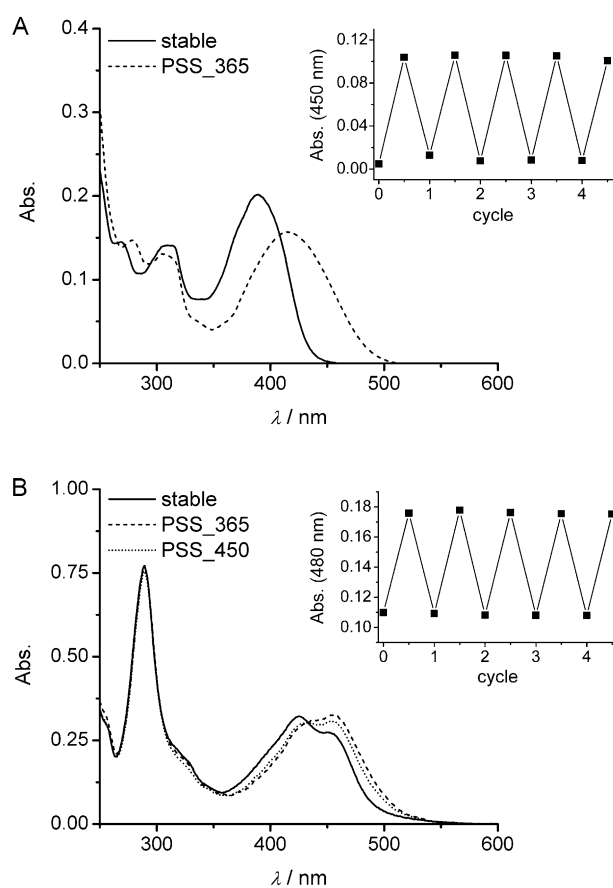


Figure 1. UV/Vis spectra before and after irradiation of A) **L2** at –20 °C and B) [Ru(bpy)₂(**L2**)](PF₆)₂ at –30 °C measured in degassed CH₂Cl₂ at 1×10^{-5} M. The insets show the change in UV/Vis absorption at 450 nm for **L2** and 480 nm for [Ru(bpy)₂(**L2**)](PF₆)₂ after several irradiation/warming cycles.

Information) verifying that the stable \rightarrow unstable conversion is a unimolecular process. When the solutions were subsequently warmed, the original UV/Vis absorption spectra were recovered, which is consistent with isomerization to the thermodynamically most stable form. This irradiation/warming could be repeated over multiple cycles without notable signs of fatigue (Figure 1, insets).

The rate of thermal isomerization was determined over a range of temperatures and the thermodynamic parameters of activation were calculated using the Eyring equation (see Table 1 and Figures S8 and S9 in the Supporting Information). The Gibbs free energy of activation ($\Delta^\ddagger G^\circ$) and corresponding half-life ($t_{1/2}$) at room temperature for **L2** are somewhat lower than the values reported earlier for **L1** ($\Delta^\ddagger G(20^\circ) =$

Table 1: Thermodynamic parameters for the thermal isomerization of unstable **L2** and [Ru(bpy)₂(**L2**)](PF₆)₂ as determined by UV/Vis spectroscopy.

	$\Delta^\ddagger H$ [kJ mol ⁻¹]	$\Delta^\ddagger S$ [J mol ⁻¹ K ⁻¹]	$\Delta^\ddagger G(20^\circ\text{C})$ [kJ mol ⁻¹]	$t_{1/2}(20^\circ\text{C})$ [s]
L2	75.6	–27.0	83.5	85
[Ru(bpy) ₂ (L2)] ²⁺	70.8	–10.9	74.0	1.7

85 kJ mol⁻¹ and $t_{1/2} = 190$ s; measured in hexane).^[20] Remarkably, $\Delta^\ddagger G^\circ$ and $t_{1/2}$ are drastically reduced when **L2** is ligated to Ru^{II}. This result indicates that metal–ligand coordination does not only allow for visible-light excitation, but may also induce an acceleration of the thermal helix inversion (THI) step.

The photoinduced formation of the unstable isomers was additionally monitored by low-temperature ¹H NMR spectroscopy (Figure S10 and S11 in the Supporting Information). The PSS₃₆₅ ratios were determined as 81:19 and 54:46 (unstable/stable) for **L2** and [Ru(bpy)₂(**L2**)](PF₆)₂, respectively. For the latter compound, correlation of the PSS₃₆₅ ratio and the 480 nm absorption increase in the UV/Vis spectrum gave an estimated PSS₄₅₀ ratio of 36:64.^[28]

DFT calculations have previously been used to provide accurate predictions of the energy barrier for the THI step of overcrowded alkene-based motors.^[29] To better understand the decrease in the $\Delta^\ddagger G^\circ$ value upon metal complexation, energy minimizations were carried out for the stable, unstable, and transition-state (TS) structures of (*R*)-**L2** and the Λ -[Ru(bpy)₂]{(*R*)-**L2**}²⁺ isomer. As reliable results have been obtained for these type of compounds using the B3LYP functional,^[29] it was chosen along with the 6-31G+(d,p):LANL2DZ mixed basis set and an IEFPCM, CH₂Cl₂ solvent model. However, it has been recently shown by Merz and co-workers that the TPSSTPSS functional gives a better approximation of the thermodynamic properties of transition-metal complexes than B3LYP.^[30] For that reason, the structures were additionally optimized using the TPSSTPSS method.

The optimized structures and their relative energies are presented in Figure 2. The stable isomers were found to exist in a twisted conformation having their methyl substituent in pseudo-axial orientation (Figure 3). The same conformation was observed in the X-ray structures of fluorenyl-derived molecular motors and is preferred over *anti* folding because of

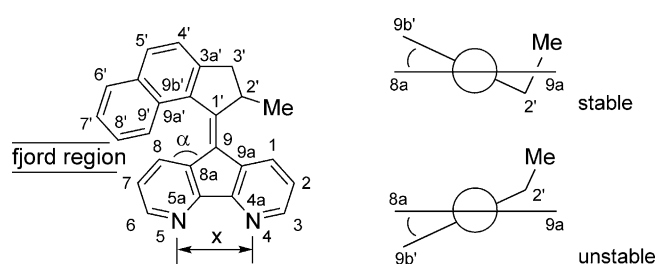


Figure 3. Line drawing of **L2** with numbering scheme and Newman projections along the C=C bond illustrating the twisted conformations.

the rigidity of the lower half.^[20] The higher energy unstable isomers also adopt the twisted conformation and, inherent to these molecular motors,^[19,20] have their methyl substituent oriented equatorially.

The DFT-optimized TS state geometry of (*R*)-**L2** shows a slightly bent diazafluorenyl lower half. Furthermore, the $\Delta^\ddagger G^\circ$ (20 °C) THI barrier (83.9 kJ mol⁻¹) calculated from B3LYP matches the experimentally obtained value (83.5 kJ mol⁻¹; vide supra) very well. For Λ -[Ru(bpy)₂]{(*R*)-**L2**}²⁺, two TS structures were found: one with a planar diazafluorenyl moiety and the other, which is 3.0 kJ higher in energy, with a similar kind of diazafluorenyl bending as in the unbound ligand (see Tables S12 and S13 in the Supporting Information). As was anticipated, the TPSSTPSS method provided the better approximation (74.1 kJ mol⁻¹) of the experimentally determined (74.0 kJ mol⁻¹) $\Delta^\ddagger G^\circ$ barrier.^[31]

The TS geometries that were optimized by using either the B3LYP or TPSSTPSS method are structurally very similar (see the Supporting Information for bond lengths and angles). Overall, some very important structural differences between **L2** and [Ru(bpy)₂(**L2**)]²⁺ can be identified, which might explain the lower $\Delta^\ddagger G^\circ$ barrier of the latter compound. For the Ru^{II} complex, the nitrogen–nitrogen distance (x) is

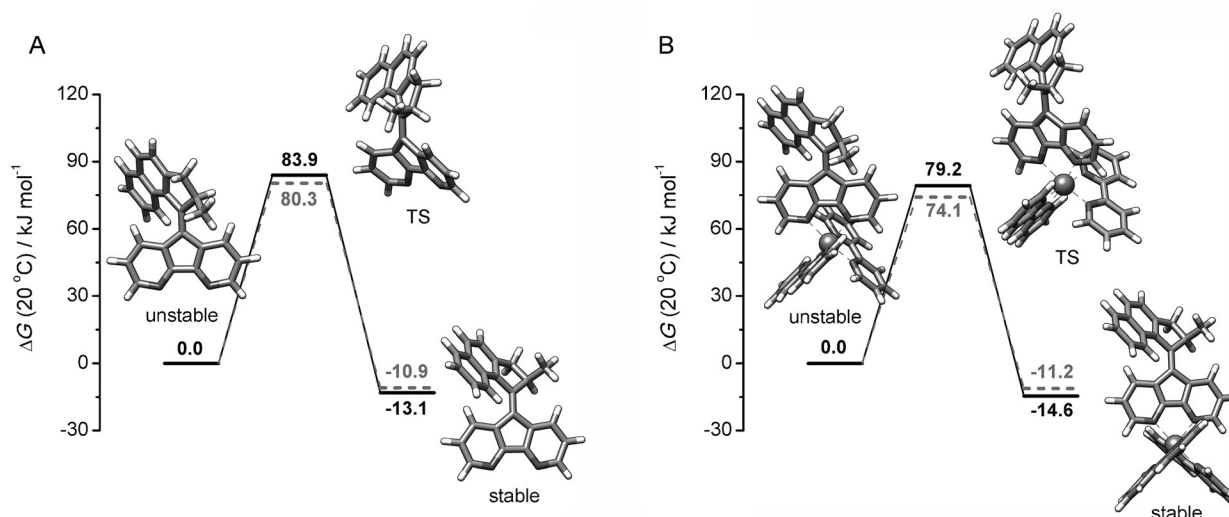


Figure 2. Plots of the relative energies between the unstable, stable and transition state geometries of A) (*R*)-**L2** and B) Λ -[Ru(bpy)₂]{(*R*)-**L2**}²⁺ optimized by DFT using either the B3LYP (solid line) or TPSSTPSS (dashed) functional. The structures depicted were obtained at the B3LYP/6-31G+(d,p):LANL2DZ level of theory.

2.80 Å, whereas it is 3.02 Å for the unbound ligand. In addition, the C₈-C_{8a}-C₉ angle (α ; see Figure 3 for the numbering scheme) is 4–5 degrees larger after metal complexation. Apparently, the diazafluorene lower half becomes slightly contracted upon coordination to Ru^{II}, which results in a decreased steric hindrance in the “fjord region” of the molecule (Figure 3).

It has been well established by our group that the speed of rotation of the molecular motor is determined by the size of the substituents in this fjord region,^[19,20] whereas electronic effects were found to have no significant influence.^[32] The present result shows that the rotary motion can also be modified through metal–ligand interactions.

In conclusion, we have presented the first molecular ligand motor **L2** for metal complexation, in which the 4,5-diazafluorene coordination motif is embedded in the motor rotary function. The photochemical and thermal isomerization behavior of this ligand is comparable to that of its fluorenyl-based counterpart **L1**. Upon ligation to Ru^{II}, the excitation wavelength could be shifted to the visible region ($\lambda = 450$ nm) and in addition, a 50-fold increase of the rotation speed was observed. Metal–ligand coordination thus offers a very practical approach to alter the photophysical and thermodynamic properties of these type of compounds. Complexation using other metal ions is currently under investigation in our laboratory. Ultimately, we aim to apply these molecular motors in photoresponsive materials operated by visible light.

Acknowledgements

Financial support from The Netherlands Organization for Scientific Research (NWO-CW, Veni grant to S.J.W.), NanoNed, the Ministry of Education, Culture and Science (Gravitation program 024.001.035) and the European Research Council (Advanced Investigator Grant, no. 227897 to B.L.F) is gratefully acknowledged. We also thank Jos C. M. Kistemaker and Prof. Dr. Wesley R. Browne for fruitful discussions.

Keywords: alkenes · metal–ligand interactions · molecular motors · photochromism · ruthenium

How to cite: *Angew. Chem. Int. Ed.* **2015**, *54*, 11457–11461
Angew. Chem. **2015**, *127*, 11619–11623

- [1] For comprehensive reviews, see: a) S. Saha, J. F. Stoddart, *Chem. Soc. Rev.* **2007**, *36*, 77–92; b) V. Balzani, A. Credi, M. Venturi, *Chem. Soc. Rev.* **2009**, *38*, 1542–1550; c) M.-M. Russew, S. Hecht, *Adv. Mater.* **2010**, *22*, 3348–3360; d) *Molecular Switches* (Eds.: B. L. Feringa, W. R. Browne), Wiley-VCH, Weinheim, **2011**; e) J. Zhang, Q. Zou, H. Tian, *Adv. Mater.* **2013**, *25*, 378–399.
- [2] For examples involving molecular motors, see: a) N. Koumura, R. W. J. Zijlstra, R. A. van Delden, N. Harada, B. L. Feringa, *Nature* **1999**, *401*, 152–155; b) D. A. Leigh, J. K. Y. Wong, F. Dehez, F. Zerbetto, *Nature* **2003**, *424*, 174–179; c) R. Eelkema, M. M. Pollard, J. Vicario, N. Katsonis, B. S. Ramon, C. W. M. Bastiaansen, D. J. Broer, B. L. Feringa, *Nature* **2006**, *440*, 163–163; d) D. Pijper, B. L. Feringa, *Angew. Chem. Int. Ed.* **2007**, *46*, 3693–3696; *Angew. Chem.* **2007**, *119*, 3767–3770; e) L. Greb, J.-M. Lehn, *J. Am. Chem. Soc.* **2014**, *136*, 13114–13117; f) Q. Li, G. Fuks, E. Moulin, M. Maaloum, M. Rawiso, I. Kulic, J. T. Foy, N. Giuseppone, *Nat. Nanotechnol.* **2015**, *10*, 161–165.
- [3] a) T. Fehrentz, M. Schönberger, D. Trauner, *Angew. Chem. Int. Ed.* **2011**, *50*, 12156–12182; *Angew. Chem.* **2011**, *123*, 12362–12390; b) W. Szymański, J. M. Beierle, H. A. V. Kistemaker, W. A. Velema, B. L. Feringa, *Chem. Rev.* **2013**, *113*, 6114–6178.
- [4] H. M. D. Bandara, S. C. Burdette, *Chem. Soc. Rev.* **2012**, *41*, 1809–1825.
- [5] M. Irie, T. Fukaminato, K. Matsuda, S. Kobatake, *Chem. Rev.* **2014**, *114*, 12174–12277.
- [6] R. Klajn, *Chem. Soc. Rev.* **2014**, *43*, 148–184.
- [7] B. L. Feringa, R. A. van Delden, N. Koumura, E. M. Geertsema, *Chem. Rev.* **2000**, *100*, 1789–1816.
- [8] D. Bléger, S. Hecht, *Angew. Chem. Int. Ed.* DOI: 10.1002/anie.201500628; *Angew. Chem.* DOI: 10.1002/ange.201500628.
- [9] For selected approaches, see: a) A. A. Beharry, O. Sadovskii, G. A. Woolley, *J. Am. Chem. Soc.* **2011**, *133*, 19684–19687; b) D. Bléger, J. Schwarz, A. M. Brouwer, S. Hecht, *J. Am. Chem. Soc.* **2012**, *134*, 20597–20600; c) S. Samanta, T. M. McCormick, S. K. Schmidt, D. S. Seferos, G. A. Woolley, *Chem. Commun.* **2013**, *49*, 10314–10316; d) C. Knie, P. Utecht, F. Zhao, H. Kulla, S. Kovalenko, A. M. Brouwer, M. Saalfrank, S. Hecht, D. Bléger, *Chem. Eur. J.* **2014**, *20*, 16492–16501.
- [10] Y. Yang, R. P. Hughes, I. Aprahamian, *J. Am. Chem. Soc.* **2012**, *134*, 15221–15224.
- [11] a) A. Osuka, D. Fujikane, H. Shinmori, S. Kobatake, M. Irie, *J. Org. Chem.* **2001**, *66*, 3913–3923; b) T. Fukaminato, T. Hirose, T. Doi, M. Hazama, K. Matsuda, M. Irie, *J. Am. Chem. Soc.* **2014**, *136*, 17145–17154.
- [12] a) P. Belser, L. De Cola, F. Hartl, V. Adamo, B. Bozic, Y. Chriqui, V. M. Iyer, R. T. F. Jukes, J. Kühni, M. Querol, S. Roma, N. Salluce, *Adv. Funct. Mater.* **2006**, *16*, 195–208; b) E. C. Harvey, B. L. Feringa, J. G. Vos, W. R. Browne, M. T. Pryce, *Coord. Chem. Rev.* **2015**, *282–283*, 77–86.
- [13] C. A. Hunter, L. D. Sarson, *Tetrahedron Lett.* **1996**, *37*, 699–702.
- [14] a) R. Sakamoto, S. Kume, M. Sugimoto, H. Nishihara, *Chem. Eur. J.* **2009**, *15*, 1429–1439; b) S. Venkataramani, U. Jana, M. Dommaschk, F. D. Sönnichsen, F. Tuzcek, R. Herges, *Science* **2011**, *331*, 445–448.
- [15] a) R. T. F. Jukes, V. Adamo, F. Hartl, P. Belser, L. De Cola, *Inorg. Chem.* **2004**, *43*, 2779–2792; b) V. W.-W. Yam, C.-C. Ko, N. Zhu, *J. Am. Chem. Soc.* **2004**, *126*, 12734–12735; c) M. T. Indelli, S. Carli, M. Ghirotti, C. Chiorboli, M. Ravaglia, M. Garavelli, F. Scandola, *J. Am. Chem. Soc.* **2008**, *130*, 7286–7299; d) K. Brayshaw, S. Schiffrs, A. J. Stevenson, S. J. Teat, M. R. Warren, R. D. Bennett, I. V. Sazanovich, A. R. Buckley, J. A. Weinstein, P. R. Raithby, *Chem. Eur. J.* **2011**, *17*, 4385–4395.
- [16] a) V. W.-W. Yam, C.-C. Ko, L.-X. Wu, K. M.-C. Wong, K.-K. Cheung, *Organometallics* **2000**, *19*, 1820–1822; b) J. L. Bahr, G. Kodis, L. de La Garza, S. Lin, A. L. Moore, T. A. Moore, D. Gust, *J. Am. Chem. Soc.* **2001**, *123*, 7124–7133; c) C.-C. Ko, L.-X. Wu, K. M.-C. Wong, N. Zhu, V. W.-W. Yam, *Chem. Eur. J.* **2004**, *10*, 766–776.
- [17] D. Martínez-López, M. Blanco-Lomas, P. J. Campos, D. Sampedro, *Tetrahedron Lett.* **2015**, *56*, 1991–1993.
- [18] V. Balzani, M. Clemente-León, A. Credi, B. Ferrer, M. Venturi, A. H. Flood, J. F. Stoddart, *Proc. Natl. Acad. Sci. USA* **2006**, *103*, 1178–1183.
- [19] a) N. Koumura, E. M. Geertsema, M. B. van Gelder, A. Meetsma, B. L. Feringa, *J. Am. Chem. Soc.* **2002**, *124*, 5037–5051; b) B. L. Feringa, *J. Org. Chem.* **2007**, *72*, 6635–6652.
- [20] a) J. Vicario, A. Meetsma, B. L. Feringa, *Chem. Commun.* **2005**, 5910–5912; b) J. Vicario, M. Walko, A. Meetsma, B. L. Feringa, *J. Am. Chem. Soc.* **2006**, *128*, 5127–5135.

- [21] A. Cossen, L. Hou, M. M. Pollard, P. V. Wesenhagen, W. R. Browne, B. L. Feringa, *J. Am. Chem. Soc.* **2012**, *134*, 17613–17619.
- [22] W. I. Smid, A. M. Schoevaars, W. Kruizinga, N. Veldman, W. J. J. Smeets, A. L. Spek, B. L. Feringa, *Chem. Commun.* **1996**, 2265–2266.
- [23] M. Querol, H. Stoekli-Evans, P. Belsler, *Org. Lett.* **2002**, *4*, 1067–1070.
- [24] P. J. Davis, L. Harris, A. Karim, A. L. Thompson, M. Gilpin, M. G. Moloney, M. J. Pound, C. Thompson, *Tetrahedron Lett.* **2011**, *52*, 1553–1556.
- [25] The term “unstable” refers to a higher-energy, metastable state and is not related to the chemical stability.
- [26] a) K. Kalyanasundaram, *Coord. Chem. Rev.* **1982**, *46*, 159–244; b) A. Juris, V. Balzani, *Coord. Chem. Rev.* **1988**, *84*, 85–277.
- [27] Identical irradiation of [Ru(bpy)₂(dafo)](PF₆)₂ (dafo = 4,5-diazafluoren-9-one) as a reference complex did not lead to any changes in absorption (Figure S3 in the Supporting Information). This observation supports the fact that the visible-light-driven process is a double-bond isomerization and is not related to ligand dissociation.
- [28] A comparable decrease in PSS ratio was observed for the isomerization of an alkoxy-substituted variant of **L1** sensitized by a Pd^{II} porphyrin (Ref. [21]). Please note that a low PSS ratio is actually not a limitation for these molecular motors since the succeeding THI step is a ‘forward’ process in the rotary cycle.
- [29] a) M. Klok, M. Walko, E. M. Geertsema, N. Ruangsapichat, J. C. M. Kistemaker, A. Meetsma, B. L. Feringa, *Chem. Eur. J.* **2008**, *14*, 11183–11193; b) A. Kazaryan, J. C. M. Kistemaker, L. V. Schäfer, W. R. Browne, B. L. Feringa, M. Filatov, *J. Phys. Chem. A* **2010**, *114*, 5058–5067.
- [30] Y. Yang, M. N. Weaver, K. M. Merz, Jr., *J. Phys. Chem. A* **2009**, *113*, 9843–9851.
- [31] The $\Delta^{\ddagger}G^{\circ}$ barrier for the Λ -[Ru(bpy)₂[(S)-**L2**]]²⁺ isomer was additionally calculated and was found to be slightly lower (72.0 kJ mol⁻¹), but still falls within an acceptable range from the experimental value (see Tables S15 and S16 in the Supporting Information).
- [32] M. M. Pollard, P. V. Wesenhagen, D. Pijper, B. L. Feringa, *Org. Biomol. Chem.* **2008**, *6*, 1605–1612.

Received: June 23, 2015

Published online: August 13, 2015